Journal of Magnetics 11(4), 170-181 (2006)

<Invited review paper>

Magnetic Tunnel Junctions with Magnesium Oxide Barriers

Taro Nagahama[1,2] and Jagadeesh S. Moodera[1]*

[1]*Francis Bitter Magnet Laboratory, Massachusetts Institute of Technology, Cambridge, MA 02139 USA*
[2]*National Institute of Advanced Industrial Science and Technology (AIST) NanoElectronics Research Institute, Tsukuba, Ibaraki 305-8568, Japan*

(Received 26 October 2006)

Spin dependent tunneling has enormously activated the field of magnetism in general, and in particular spin transport studies, in the past ten years. Thousands of articles related to the subject have appeared with many fundamental results. Importantly, there is great interest in their potential for application. There was another surge of activity in this field since the past five years - created by the theoretical prediction of a large tunnel magnetoresistance that arises due to band symmetry matched coherent tunneling in epitaxial magnetic tunnel junctions with (001) MgO barrier and experimentally well demonstrated. This further development in the field has boosted the excitement in both fundamental science as well as the possibility of application in such as magnetic random access memory, ultra sensitive read heads, biosensors and spin torque diodes. This review is a brief coverage of the field highlighting the literature that deals with magnetic tunnel junctions having epitaxial MgO tunnel barriers.

Keywords : spin dependent tunneling, magnesium oxide barriers, tunnel magnetoresistance, spin polarization, coherent spin transport

1. Introduction

Extensive activity in the area of spin tunneling with magnetic tunnel junctions (MTJs) has opened an exciting field of research and led to many outstanding fundamental results. Since the demonstration of a large tunnel magnetoresistance (TMR) in MTJs in 1995 there have been thousands of articles on this topic [1]. Great many technological applications for magnetic storage such as read heads in the hard drives and magnetic random access memory (MRAM) elements are becoming a reality based on MTJs [2]. Super sensitive detectors for biological applications is another area that is capturing the attention [3].

The field of spin polarized tunneling (SPT) began in the early 70s with the pioneering studies of Meservey and Tedrow, where they showed that the tunneling electrons coming from a ferromagnetic electrode showed spin polarization (P) [4]. The detection was done with a superconductor that had its quasi particle density of states Zeeman split in a large applied magnetic field. Most importantly their work showed the spin conservation in the tunneling process, which is the main basis for the MTJ studies that was rigorously pursued since 1995 [5, 6]. Most of the fundamental as well as technological developments using MTJs have been with Al_2O_3 tunnel barrier between various ferromagnetic (FM) electrodes, whereas in a few cases other barriers such as Ga_2O_3 and $SrTiO_3$ have been used successfully as well [7, 8]. Extensive work has been published with amorphous Al_2O_3 tunnel barriers; with CoFeB electrodes, with the highest obtained TMR being 70% at RT and 113% at LHe temperatures [9], corresponding to a P_{CoFeB} of 60% at 1 K. In these amorphous barriers the momentum conservation and coherent spin transport are absent.

2. Theoretical

There was a surge in the activity after the theoretical prediction of achieving a huge TMR with epitaxial MTJs with crystalline MgO barrier. This was based on the wave function symmetry matching at the FM-insulating barrier interfaces, such as Fe/MgO. Mavropoulos *et al.* [10] by considering the complex band structure of MgO in epitaxial FM/I/FM system predicted that the Δ_1 (majority

*Corresponding author: Tel: +1-617-253-5423,
Fax: +1-617-253-5405, e-mail: moodera@mit.edu

© 2006 Journal of Magnetics

spin band) in Fe(001) had the slowest decay rate inside MgO(001) barrier. Hence the tunneling was to be dominated by this band at the Γ point that could lead to a large TMR. Although most of their theoretical treatment was for semiconducting barriers such as ZnSe, Ge etc, with the results they obtained for ZnSe barrier, however, they could see the importance of Fe/MgO/Fe epitaxial junction for obtaining a very large TMR, a first such prediction.

This was followed by the two important theoretical papers independently by two different groups, Butler *et al.*, and Mathon and Umerski; both dealing with epitaxial Fe(100)/MgO(100)/Fe(100) system [11, 12]. For example, Butler *et al.* [11] from first principles calculations showed that the symmetry of both the propagating states in the electrodes and of the evanescent states in the barrier material are crucial in determining the tunneling conductance. Specifically, tunneling conductance and TMR in the above epitaxial system were strongly controlled by the symmetry matching of the Bloch states in the FM electrodes and the evanescent states in the barrier. They found the state with Δ_1 symmetry coupled effectively from the Fe into the MgO. This gave rise to different decay rates of the Bloch states of different symmetry inside the barrier, whereby the majority and minority channels showed very different tunneling probability. The result is that a large difference in the conductance for the two spin channels occurs: the primary conductance is via Δ_1 Bloch states with $k_{\parallel} = 0$ for the majority electrons whereas the interface resonance states controlled the minority channel conductance. Majority Bloch states with Δ_1 symmetry in the Fe electrode decay as evanescent states with Δ_1 symmetry in MgO, whereas minority Bloch states with Δ_5 symmetry decayed strongly in the barrier. The tunneling DOS in Fig. 1, shows the dominance of majority spin channel conductance. This led them to predict over 1000% TMR in Fe/MgO/Fe epitaxial junctions. Similarly, in excess of 1000% TMR was also predicted by real-space Kubo formula using tight binding bands and *ab initio* band structure of Fe and MgO in the theory put forward by Mathon and Umerski [12].

The symmetry driven preferential tunneling of Δ_1 majority electrons can show positive and significantly higher P coming out of Fe(100)/MgO(100) when it reaches the second electrode – *spin filtering* of sorts [11, 12]. Butler *et al.* also remark that the tunneling rates are higher if similar or identical states are present on both sides of the barrier. From this theoretical model it was seen that the temperature dependence of tunnel junction resistance (R_J)

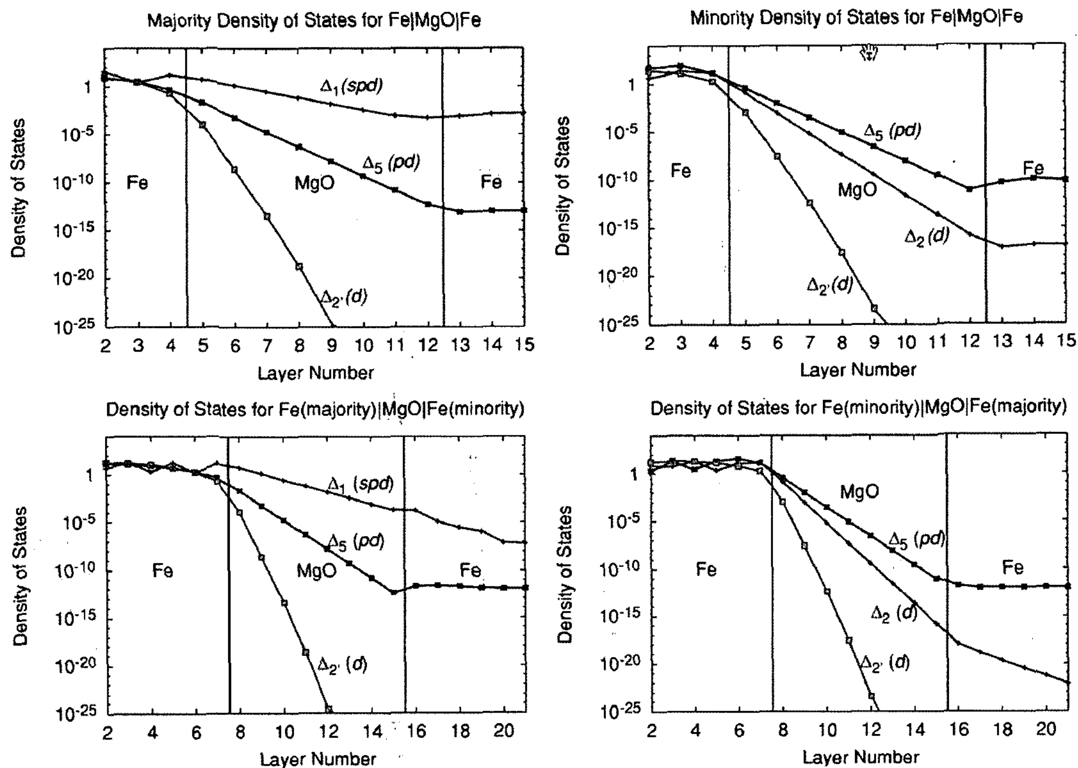

Fig. 1. Theoretical tunneling density of states for $k_{\parallel} = 0$ in Fe(100)/MgO(100)/Fe(100) junction. Top two plots are for parallel and bottom two are for antiparallel magnetization configuration. The left panel is for majority whereas the right panel is for minority spin states. Slow decay of Δ_1 majority (spd) states, compared to other states in the MgO barrier is seen which is responsible for high TMR. From Ref. 11.

Table 1. Tunneling conductivity (in $1/\Omega{\cdot}m^2$) for various spin channels for the Co/MgO/Co and FeCo/MgO/FeCo tunnel junctions. Each junction contained eight atomic layers of MgO. Resonant state contributions to the minority spin channel have been removed. Results for Fe/MgO/Fe are also listed for comparison. The electrode materials were all assumed to have the bcc phase and all interfaces normal to the (100) direction. From Ref. 13.

Spin Alignment	up-up	down-down	up-down (down-up)	ρ_P/ρ_{AP}
FeCo/MgO/FeCo	1.19×10^9	2.55×10^6	1.74×10^6	340.5
Co/MgO/Co	8.62×10^8	7.51×10^7	3.60×10^6	130.2
Fe/MgO/Fe	2.55×10^9	7.08×10^7	2.41×10^7	54.3

and TMR mostly come from minority spin tunneling.

The above calculations of tunnel conductance was later extended by Zhang and Butler to other epitaxial systems, bcc Co(100)/MgO(100)/bcc Co(100) and FeCo(100)/MgO(100)/FeCo(100) [13]. In these MTJs the predicted TMR was several times larger than for Fe/MgO/Fe epitaxial junctions, since no minority Bloch states with Δ_1 symmetry is present for antiparallel alignment. This gave rise to complete reflection of all states when the two magnetizations (M) are antiparallel, leading to much larger conductance ratio for Co and FeCo based MTJs. The predicted tunnel conductances are listed in Table 1.

In all of the above theoretical treatments perfect epitaxy and clean interfaces were assumed. However, the same authors observed that tunneling magnetoconductance greatly reduced if a layer of FeO formed at the Fe/MgO interface. This is due to the bonding of Fe and O reducing the conductance for M parallel compared to the antiparallel case. The TMR was observed to decrease exponentially with increasing FeO formation at the interface. This was further studied by Yu and Kim for the MgO/Fe(001) system with excess Mg or O at their interface [14]. Having Mg rich had cleaner interface whereas O-rich condition yielded MgO/FeO/Fe interface significantly affecting the electronic and magnetic properties of the bilayer system. Introducing disorder at the Fe/MgO/Fe interface, calculation by Heiliger *et al.* observed that TMR reduced, giving rise to positive and negative TMR ratios and even showing sign reversal with bias [15].

3. Experimental

MTJs with nonepitaxial MgO barriers were first studied by Moodera and Kinder [16], soon after the success of MTJs with Al_2O_3 barrier. Here MgO was formed by depositing an ultra thin layer of Mg metal and subsequently oxidizing it with O plasma. These junctions, with polycrystalline FM electrodes and nearly amorphous MgO, such as Co/MgO/CoFe, gave only a moderate TMR of ~20-25% at room temperature and ~33% at LHe temperatures. Five years later the situation began to shift when epitaxial FM electrodes and MgO barriers were investigated by others. The first successful results on all epitaxial Fe/MgO/FeCo tunnel junctions on MgO buffered GaAs substrates were reported by Bowen *et al.* in 2001. [17] They observed a TMR of 60% at 30 K, decreasing to 27% by 300 K. They correctly pointed out that spin polarization depended on the actual electronic structure of the barrier/FM interface, in this case Fe/MgO and from the bias dependence it was concluded that predominantly *s*-electrons contributed to tunneling. These authors were aware of the theoretical prediction of Butler *et al.* [11] regarding the dominance of Δ_1 symmetry band. It appears that Bowen *et al.* did not anneal their junctions, which is required to obtain high TMR as was observed by others later.

Subsequently higher TMR was obtained by Faure-Vincent *et al.* in epitaxial Fe/MgO/Fe junctions with slightly thicker MgO layers (2.5 nm) as was predicted by both theories as discussed above: for example, a TMR of 67% at RT and 100% at 80 K were observed [18]. These authors attributed the relatively lower value of TMR compared to theoretical expectation to the presence of a thin layer of FeO at the bottom Fe/MgO interface, which was also supported by the high asymmetry in the conductance vs bias data. Another observation was the significantly higher temperature dependence of R_J in the antiparallel magnetization configuration, attributed to stronger scattering of minority spins as predicted by the theory.

Although several independent theoretical calculations showed that large TMR is obtainable with epitaxial Fe/MgO/Fe junctions, and some of the experimental reports showed signs of large values, it was nontrivial to realize TMR values anywhere near the expected numbers. Among many limiting factors, loss of coherence at Fe/MgO interfaces, maintaining smooth epitaxial growth of the layers, interfacial oxidation of Fe layers etc have detrimental effect on the band symmetry matching needed at the interface. This resulted in low TMR. Optimum annealing of the layer stack turned out to be crucial. For example, during the deposition of MgO, it decomposes into Mg and O which can oxidize the surface of the bottom Fe(001) electrode, leading to the formation of FeO at the interface which reduced the tunnel current spin polarization and also destroying the interfacial symmetry matching [19].

Meyerheim *et al.* [19] investigated their MTJs by surface X-ray diffraction and found FeO layer at the interface between MgO and Fe(001) electrode. Wolfhekel *et al.*

[20] and Klaua *et al.* [21] fabricated MgO tunnel barrier on the Fe(001) whiskers and the single crystal Fe(001) disks and investigated structure and tunnel characteristics in detail using STM. In these earlier trials to make MgO junctions, the junctions showed tunneling I-V characteristics, but had zero or small TMR. The detrimental effect of this FeO layer at the interface has been mentioned above.

The increased chance of achieving a large TMR began to show up by early 2004 with the publication of Yuasa *et al.* [22]. In Fe/MgO/Fe junctions they obtained 88% at RT and 146% at 20 K. The bias dependence was highly asymmetric: when the top electrode was positive the V_{half} (bias at which TMR reduces to half of its zero bias value) was an impressive 1250 mV. This is ~ three times higher than that for Al_2O_3 barrier MTJs and clearly showing signs towards application. From their TMR versus bias data it appears that the 'low' value of TMR arises due to the bottom interface being imperfect – possible FeO formation. Several months later, two reports appeared simultaneously, – by Yuasa *et al.* [23] and Parkin *et al.* [24], showing a factor of two or greater increase in TMR value at RT. It was correspondingly higher at LHe temperatures as well. Since 2005 many other reports have appeared, with TMR reaching near 500% at RT and > 800% at LHe temperatures. From the temperature dependence of R_J which is rather small for parallel and considerable for antiparallel configuration of M, it can be seen that the increase in TMR at low T comes from the latter. This is observed in all of the MgO junction reports that show good TMR values, nearly irrespective of the FM electrodes used.

Yuasa *et al.* further improved on the earlier observations by carefully fabricating better quality Fe(001)/MgO(001)/Fe(001) tunnel junctions using MBE, and observed a TMR of 180% at room temperature and 240% at 20 K as shown in Fig. 2(a) [23]. The TEM image of their junctions (Fig. 2(b)) shows clear (001) crystal orientation through the entire junction structure. Such single-crystal MgO tunnel barrier, as expected by theory, filters the Δ_1 electrons giving rise to the high TMR ratio. According to the theory [11, 12], the TMR ratio increases with increase of MgO barrier thickness. This is because the thicker tunnel barrier filters out the electrons whose momentum vector deviates from the normal to the barrier. Also for thinner barriers there can be some contribution from other bands, which decays off to negligible levels when MgO gets thicker. This is seen in the above experiment where the TMR ratio increased as MgO thickness increased, shown in Fig. 3. Additionally, interesting oscillatory behavior as a function of the MgO thickness, with a period of 0.3 nm is observed. The authors note that these oscillations are not due to the structure since the lattice constant of MgO(001) is 0.22 nm, whereas it possibly comes from the complex wave vector of tunneling electrons in MgO and "hotspot" of the transport for minority electrons. This is yet to be put on a firm ground. The other important observation was that the TMR ratio decreased more gradually with the bias than Al_2O_3 barrier junctions, with V_{half} of over 1 V.

Similarly, Parkin *et al.* obtained high TMR values in tunnel junctions with MgO tunnel barriers [24]. Their samples were grown by sputtering and used FeCo alloy electrodes to demonstrate a TMR of 140~220% at room temperature and about 290% at 5K. TEM studies showed crystallographically textured MgO(001) barrier and polycrystalline electrodes. Observed TMR was independent of MgO thickness in the range they studied. The V_{half} for

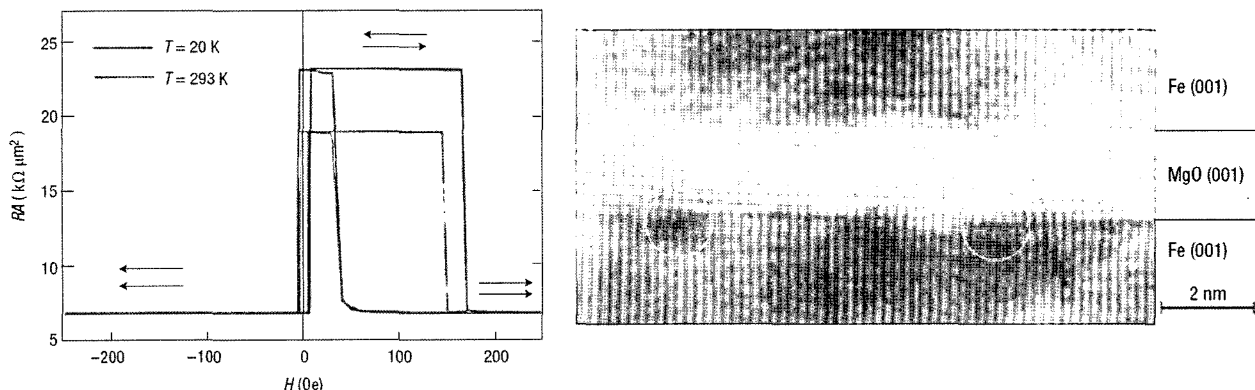

Fig. 2. From Ref. [23]. a) Tunnel magnetoresistance of Fe(001)/MgO(001)/Fe(001) junctions. The resistance-area product *RA* plotted as a function of H showing magnetoresistance (measured with 10 mV bias voltage) at T = 293 K and 20 K for a 1 μm × 1 μm area junction with 2.3 nm thick MgO barrier. Arrows show the magnetization configurations of the top and bottom Fe electrodes. The TMR ratio was 180% at 293 K and 247% at 20 K. b) TEM image of a single-crystal MTJ with the Fe(001)/MgO(001)(1.8 nm)/Fe(001) structure. Lattice dislocations are circled. With proper annealing the dislocation density was observed to be reduced.

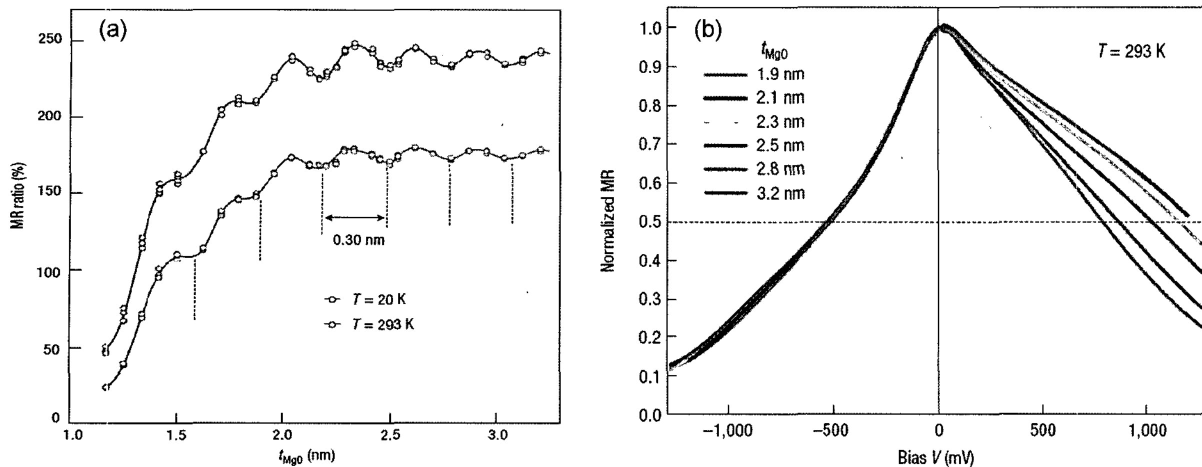

Fig. 3. From Ref. [23]. a) TMR ratio at T = 293 K and 20 K for Fe(001)/MgO(001)/Fe(001) junctions as a function of MgO thickness, showing oscillations that are yet to be understood. b) Normalized TMR as a function of junction bias voltage-dependence of the TMR effect at room temperature for Fe(001)/MgO(001)/Fe(001) tunnel junctions with various MgO thickness. The direction of bias voltage is defined with respect to the top electrode.

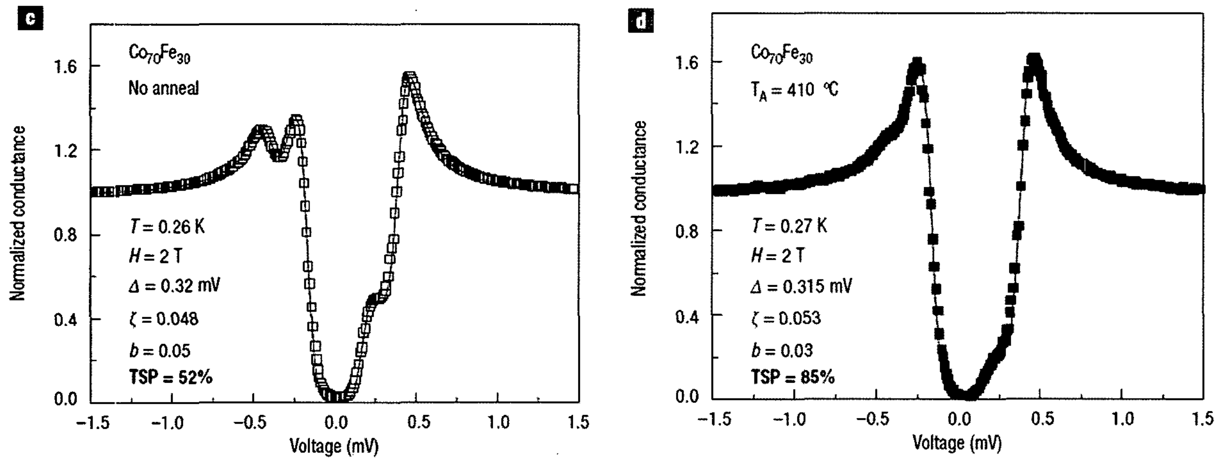

Fig. 4. Measurement of tunneling spin-polarization using Meservey Tedrow technique. Conductance versus bias voltage curves (symbols) and fits (solid lines) for STS junctions with superconducting counter electrodes of $Al_{96}Si_4$. The values for the TSP were extracted by fitting the data curves. The increase in P after annealing at high temperature can be observed. From Ref. [24].

their junctions was much smaller, between 0.3 and 0.6 V showing nonideal interfaces. Here it was also pointed that they consistently observed much lower TMR for Fe electrodes. The significantly larger temperature dependence of R_J for antiparallel magnetization orientation compared to the parallel case was attributed to magnetic disorder and thermal excitation. These authors measured the spin polarization of the tunnel current using a superconducting counter electrode, by Meservey-Tedrow technique [4]. A spin polarization of 85% was observed for $Co_{70}Fe_{30}$ at 0.3 K using $Co_{70}Fe_{30}/MgO/Al_{96}Si_4$ junctions after annealing whereas it was 52% before annealing as shown in Fig. 4.

Although the MgO based MTJs show very high TMR, the theories predict larger values than experiment, even more so for bcc Co or CoFe electrodes (see Table 1) [13]. In order to observe larger TMR, Yuasa *et al.* fabricated the MTJs with bcc-Co electrode [25]. These junctions exhibited TMR of up to 410% at room temperature and 507% at 20 K as shown in Fig. 5. The key to this extremely high value, they attributed, as apparently due to the band structure of bcc-Co. In bcc-Co majority band in the [001] direction, no band exists except the Δ_1 majority band at Fermi level. This band structure prohibits the tunneling in antiparallel configuration. As a result the conductance in antiparallel configuration is minimum, leading to a large enhancement of TMR.

It may be pointed, however, that in the experiments of Yuasa *et al.* there is also the possibility of interfacial layer

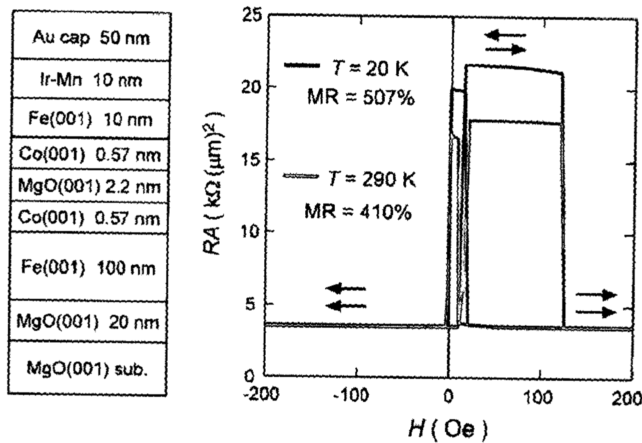

Fig. 5. Cross-section structure of fully epitaxial Co(001)/ MgO(001)/Co(001) magnetic tunnel junction (MTJ) with metastable bcc Co(001) electrodes (left-hand side) and magnetoresistance curves at bias voltage of 10 mV for the MTJ with MgO thickness of 2.2 nm (right-hand side). The red and blue curves represent magnetoresistance curves at 290 K and 20 K, respectively. Arrows represent magnetization alignments. From Ref. 25.

to be bcc FeCo alloy instead of bcc Co. This is because the samples were annealed at high temperatures and thick layers of Fe were present adjacent to the ultra thin Co layers (see sample stack on the left in Fig. 5). Nevertheless the high TMR is significant since epitaxial FeCo alloy with single crystalline MgO barrier is also predicted to yield high TMR (Table 1). It is worthwhile to note that in this work, the deduced spin polarization (using Julliere's model) showed only 3% decrease from LHe temperatures to RT.

According to the theories, single-crystalline FM electrode is needed to show the high TMR because well-defined, clean and atomically ordered interfacial structure was needed to create the perfect band matching for the large TMR. These conditions become rather restrictive if they have to be technologically applicable. One has to go for those materials whose lattice constants match with that of MgO. However, from the viewpoint of application various materials are necessary to fabricate devices, e.g. magnetic pinning layer and synthetic antiferromagnetic layer. The biggest and pleasant surprise came unexpectedly with the observation of 230% TMR at RT in CoFeB/MgO/CoFeB MTJs by Djayaprawira *et al.* [26]. It was a welcome breakthrough for applications because the structure of CoFeB electrodes was amorphous, greatly extending the possibility of FM materials one could use for MTJs and still have very large TMR. In these junctions, it was observed that highly textured (001) MgO layer grew on amorphous CoFeB. Annealing was necessary to obtain

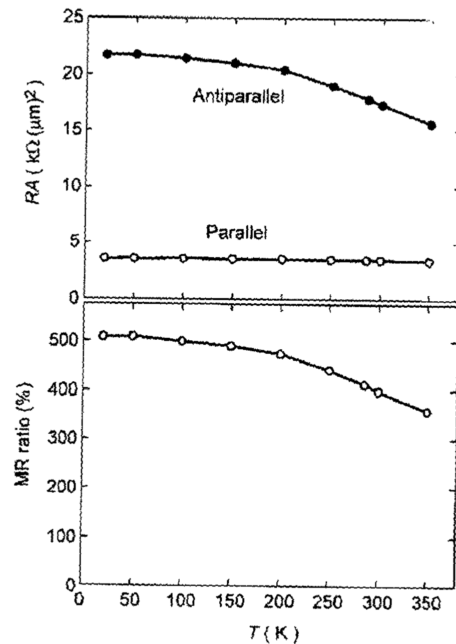

Fig. 6. From Ref. [25]. (a) Temperature dependence of resistance-area (*RA*) product in parallel (open circles) and antiparallel (solid circles) magnetization alignment for a Co(001)/ MgO(001)/Co(001) junction with MgO barrier thickness of 2.2 nm. (b) Temperature dependence of TMR for the same junction as above.

high values of TMR. In these early measurements it was thought that CoFeB remained amorphous after annealing and still one was able to obtain large TMR which in itself was a big surprise. As seen later (discussed below) it is not quite true.

High temperature annealing of the MTJs in all cases has been found to be absolutely important in achieving high TMR, with optimum annealing temperature (T_a) above 350°C. The general consensus is that during annealing MgO becomes better crystalline and (001) oriented, whereas the interface also becomes cleaner (O taken away from Fe into MgO). A systematic study of the changes in TMR and RA (resistance × area) product for parallel and antiparallel M as a function of annealing temperature for three types MTJs were studied by Ikeda *et al.* [27]. This is shown in Fig. 7, for data taken at RT. The variation of spin polarization deduced from the TMR values using Julliere's formula, as a function of T_a is also shown. One can see that the TMR starts out low, < 30%, for as grown MTJs and increases with T_a, reaching the highest values (for $Co_{40}Fe_{40}B_{20}$ electrodes, reaching 355% at RT and 578% at 5 K) at some optimum T_a (~400°C), beyond which it decreased. Interestingly RA (parallel) reduces whereas RA (antiparallel) increases with T_a up to this optimum temperature. From the XRD structural studies

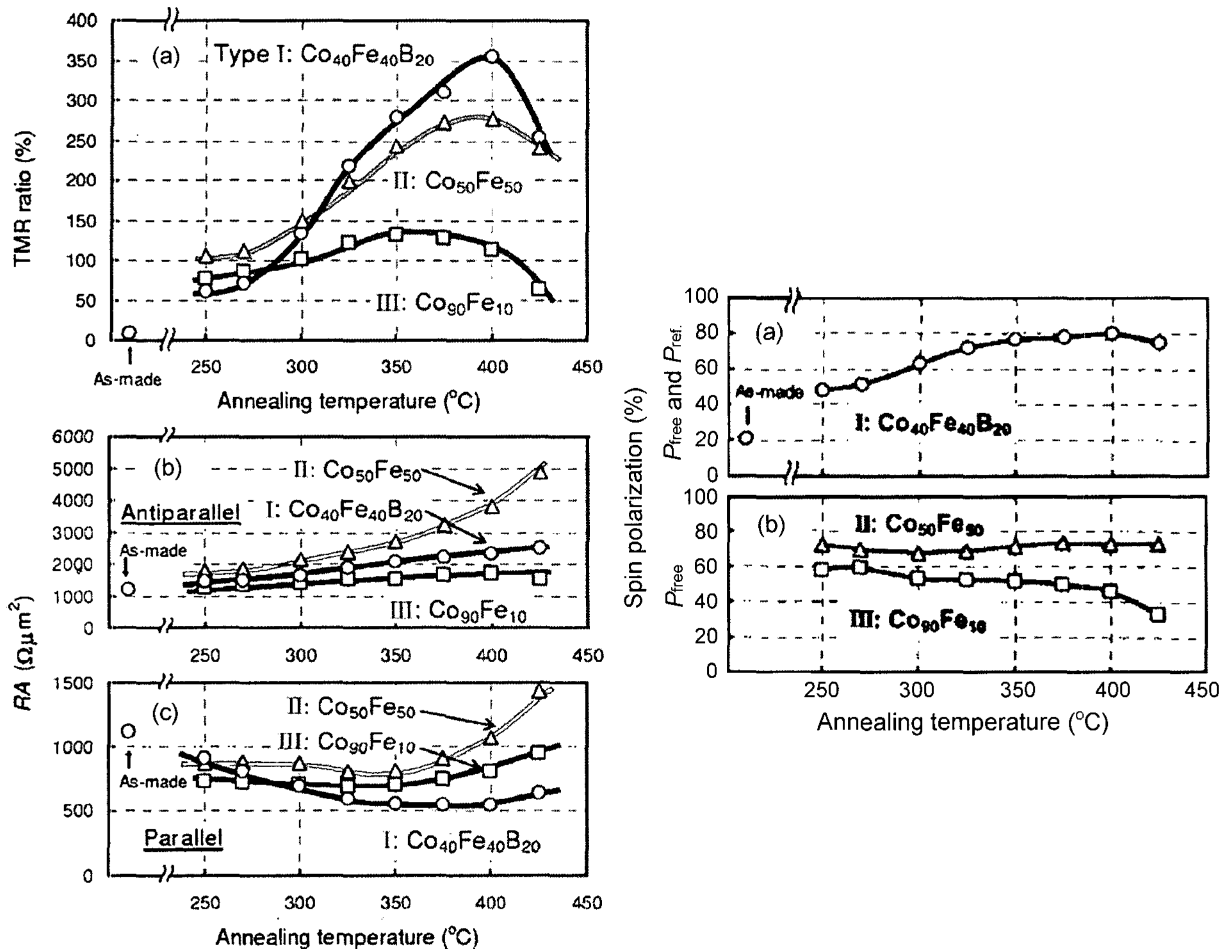

Fig. 7. From Ref. [27]. Left panel: Annealing temperature dependence of (a) TMR ratio, (b) *RA* in parallel, and (c) antiparallel magnetization configurations at RT for the MTJs with $Co_{40}Fe_{40}B_{20}$ (Type I), $Co_{50}Fe_{50}$ (Type II), and $Co_{90}Fe_{10}$ (Type III) free layers. Right panel: Annealing temperature dependence of tunneling spin polarization (a) P_{free} and $P_{ref.}$ for $Co_{40}Fe_{40}B_{20}$ free and reference layers in type I, and (b) P_{free} for $Co_{50}Fe_{50}$ free layer in type II and $Co_{90}Fe_{10}$ free layer in type III.

they found that amorphous $Co_{40}Fe_{40}B_{20}$ layer crystallized to bcc structure beyond 250°C, whereas $Co_{50}Fe_{50}$ was always in bcc form and $Co_{90}Fe_{10}$ formed in fcc structure. This supported the changes in TMR and P values with T_a. In other words, annealing is highly beneficial for coherent tunneling, and spin filtering of the spin bands by the MgO barrier is greatly increased (Δ_1 band tunneling), improving the interfacial structure, sharpness and atomic ordering (as is seen below).

The above same group very recently [27] carried out further careful annealing studies. They found a TMR of 472% at RT, increasing to 804% by 5 K in pseudo-spin valve $Co_{20}Fe_{60}B_{20}$/MgO/$Co_{20}Fe_{60}B_{20}$ junctions annealed at 450°C. These are the highest values up to date. In this recent work they also observed that diffusion of Mn and Ru layers (used for exchange biasing) in larger amounts towards the barrier appears to be the major cause for TMR decrease at high T_a rather than crystallization of the FM electrodes or lowered H_{exch}, although the weakening of exchange bias makes the AP alignment more difficult.

There have been several microscopic studies of the growth and interfaces in the MgO junctions [22–29]. Bae *et al.* carried out interesting cross sectional TEM studies along with XPS study to determine the structure and compositional changes at the interface of CoFeB/MgO/CoFeB before and after annealing [28]. This study clearly showed the changes that occur during high temperature annealing. The as-deposited amorphous CoFeB film actually crystallized at the interface and the MgO itself was (001) oriented. What is even more remarkable was that the presence of the FeO at the bottom interface in as-deposited junctions disappeared after annealing. They also observed B partly diffusing into MgO and getting oxidized after annealing. [Heat of formation for B_2O_3, Fe_3O_4 and CoO respectively are 1278, 1014 and 253 kJ/mole.] In case what is left at the interface with the MgO

is more or less CoFe, then it can explain the large TMR, which according to theory is what is expected. This supports the view that annealing has beneficial effects in MgO based junctions: i) interfaces become sharper and cleaner, ii) spin polarization increases, and iii) the correct crystal structure forms that allows for the Δ_1 band spin up electrons to tunnel freely, thereby giving rise to high TMR. Lee *et al.* found that in CoFeB/MgO/CoFeB junctions, pinning the bottom FM using a Ru layer helps in achieving even better TMR and also that the junctions were thermally stable to above 450°C [29].

One of the materials combination that might be exciting for MTJ would be Heusler compound FMs for the electrodes with MgO barriers. There are reports of full epitaxial junctions such as HC/MgO/$Co_{50}Fe_{50}$ where HC is the Heusler compound, Co_2MnGe or $Co_2Cr_{0.6}Fe_{0.4}Al$ [30]. Although Co_2MnGe junctions had low TMR at RT, with $Co_2Cr_{0.6}Fe_{0.4}Al$ 90% TMR was seen at RT and increasing to 240% at 4.2 K. In the case of Co_2MnGe there was strong bias dependence, and showed change of sign of TMR at certain bias range both at RT and 4.2 K, which was interpreted as showing features in the spin density of states in Co_2MnGe. Given the sensitivity of the energy gap in the minority spin band to composition and site occupancy in Heusler alloys, especially at the interfaces this kind of explanation may be taken cautiously. In fact earlier the same group had much lower TMR when the composition was not properly controlled in the case of $Co_2Cr_{0.6}Fe_{0.4}Al$ electrode junctions. Thus MTJs with HC may yet to be optimized and there is promise of much larger effects to be seen.

A remarkable point of the MgO based MTJs is that the R_JA product is few k$\Omega\cdot\mu m^2$ or even less than hundred $\Omega\cdot\mu m^2$ for thinner barriers, without resorting to ultra thin barriers. This is order of magnitude lower than with Al_2O_3 barriers, the main reason being the lower barrier height of epitaxial MgO junctions. For instance in a detailed study by Yuasa *et al.* [23] using MgO thickness ranging from ~1.2 nm to 3.5 nm clear exponential dependence of RA with MgO thickness was seen; the barrier height (ϕ) derived using WKB approximation or by Simmons model was close to 0.4 eV. These authors attributed the lower value of ϕ to the presence of charge neutral O vacancies in MgO barrier. If the effective mass of the electron in MgO is taken as 0.5 m_e, then ϕ goes up to ~0.6 eV. For polycrystalline barriers the values are higher, about 0.9 to 1.1 eV [16, 17, 24]. For a high quality crystalline MgO grown on Fe whisker Wolfhekel *et al.* [20] determined by STM studies a ϕ of 3.7 eV which is what one expects for MgO which has an energy gap of 7.8 eV, whereas in some regions of MgO they observed smaller values which

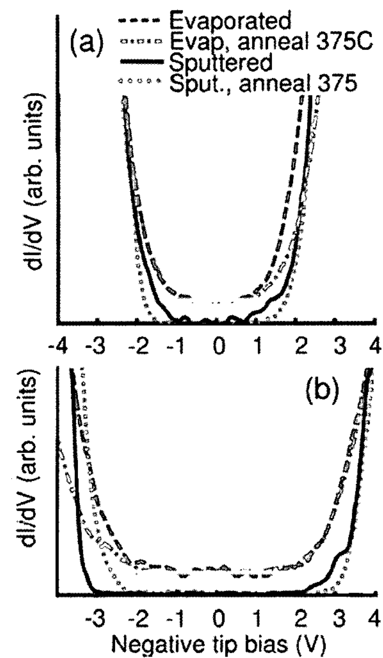

Fig. 8. Conductance measurement of MgO barriers using in situ STM. DOS measurements for several 20 Å film prepared under different methods (a). Sputtering produced a band gap of ~1.5 eV, which increases to ~2.5 eV after annealing by reducing vacancy-defect sites. E-gun evaporation results in band gaps that did not improve upon annealing. (b) Measurements for 30 Å films show that as the surface moves away from the strained, disordered Fe/MgO interface the vacancy-defect density drops and the band gap increases. From Ref. 31.

was attributed to the presence of localized states in MgO. In crystalline MTJs, if the noticeably lower value of the barrier height of MgO is due to O defects, it is interesting to note that they are still significantly present after annealing and also that the spin tunneling does not seem to be seriously affected. The apparent large difference in ϕ, in crystalline MgO in the two cases discussed above may be due to the difference in the top electrode – in one case it is epitaxial Fe film where as it is a W tip in the other case. This perhaps points to the role of effectively coupling of Δ_1 symmetry state from the Fe into with the MgO in epitaxial system and the importance wave function symmetry of the receiving electrode or in other words the absence of similar states to accept the tunneling electrons [11].

After the discovery of very high TMR in MTJ with MgO barrier, many physical properties of these junctions were investigated. In order to understand the low barrier height and the sensitivity of TMR to the quality of the interface, Mather *et al.* [31] studied in situ the band gap and defect states in ultrathin MgO(001) tunnel barrier by scanning tunneling spectroscopy (STS). The MgO tunnel

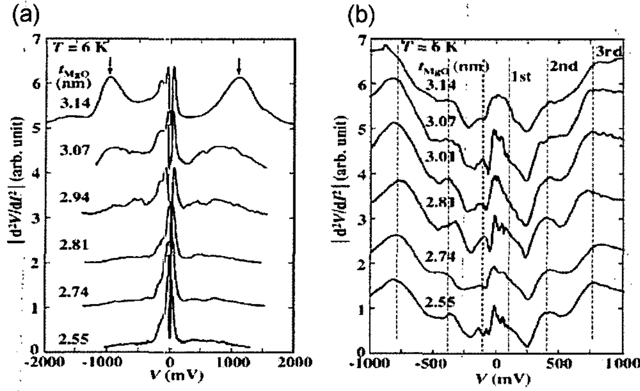

Fig. 9. IET spectra in antiparallel (a) and parallel (b) magnetization configurations. Spectra are measured for various thickness of MgO tunnel barriers, t_{MgO}. Each spectra is shifted for clarity. From Ref. 32.

barriers were grown by e-beam evaporation or magnetron sputtering. They found that a the broad band tail exists in the band gap of MgO, depending on the MgO thickness and deposition process (Fig. 8). The band tails were attributed as due to O and Mg vacancies in the oxide barrier, and that the deposition process and thermal annealing could control the density of the vacancies.

Inelastic tunnel (IET) spectroscopy measurements were carried by Ando *et al.* for Fe(001)/MgO/Fe(001) junctions to look for Fe band features [32]. In the antiparallel configuration, the IET spectra showed a large peak at ~1000 mV, which was attributed to the Δ_1 band edge of minority spin electrons (Fig. 9(a)). They also found oscillatory behavior in IET spectra in the parallel configuration (Fig. 9(b)). Although the origin of these oscillations is unclear so far, the authors suggested that it could be the effect of "hot spots" of minority spin tunneling.

With the success of obtaining a highly ordered and sharp interface structure of Fe/MgO it is now possible to study other exciting fundamental physics with spin as a probe. Having a large TMR is beneficial in this exploration. Two such studies are described below. In a careful study, interfacial resonance state in the minority spin d band of Fe (100) has been observed in epitaxial Fe/MgO/Fe junctions by Tiusan *et al.* [33] A negative TMR is observed beyond certain bias voltage as shown in Fig. 10. These authors explain the change in the sign of TMR at ~0.2 V and also the crossover in the conductance for parallel and antiparallel configurations at the same voltage as follows. The consequence of the resonance states was that when the junction was biased at this energy the increased tunneling into these states compensated the spin filtering that occurs for the Δ_1 band and thus reversing the sign of TMR. They found that in order for this resonant

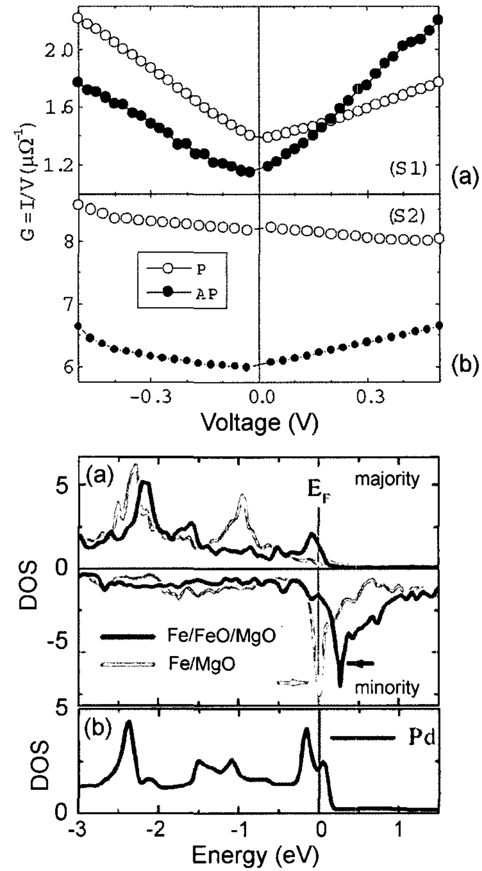

Fig. 10. From Ref. 33. a). Bias dependence of TMR measured in samples (S1 = Fe/MgO/Fe) and (S2 = Pd/Fe/MgO/Fe), respectively. Insets: Positive TMR versus magnetic field *H* [TMR(H)] curve measured at $V = -0.1$ V ($V+$ = top MTJ electrode); negative TMR(H) curve measured at $V = +0.5$ V ($V+$ = bottom MTJ electrode). b) Tunnel conductance versus voltage curves for samples (S1) (a) and (S2) (b) measured in parallel (open symbols) and antiparallel (closed symbols) magnetic configurations of the MTJ electrodes, respectively. c) (a) Calculated local spin-polarized DOS for the interfacial Fe in Fe/MgO/Fe and Fe/FeO/MgO/Fe stacks. The arrows indicate the interfacial resonance in the minority DOS of Fe. (b) The total DOS of bulk Pd.

state to exist it had to couple to the bulk, 50 nm thick, Fe layer. Whereas when this coupling was broken with a thick Pd layer (with no states present at these energies) below the 2 nm Fe layer, this resonant assisted additional conductance was not present for antiparallel configuration. They supported their data and interpretation by electronic structure calculation for Fe and Pd layers as shown in Fig. 10.

Nozaki *et al.* [34] investigated the influence of layered nanoscale Fe islands as a middle layer on the spin-dependent tunneling conductance properties in fully epitaxial double MgO barrier magnetic tunnel junctions. The junc-

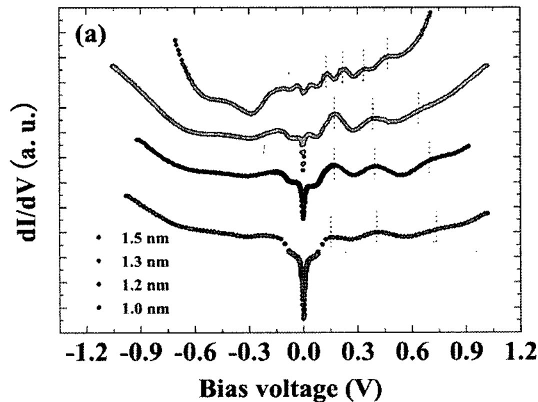

Fig. 11. (a) Dependence of tunnel conductance in parallel magenetization configuration, at 4.5 K for various middle magnetic layer thickness (t) in Fe(50)/MgO(2)/Fe(t)/MgO(2)/Fe(15) junctions. The numbers in parenthesis is in nanometers. From Ref. 34.

tion structure used was epitaxial Fe/MgO/Fe (t)/MgO/Fe, where t indicates the thickness of the middle Fe layer (1-1.5 nm). As a function of the bias voltage clear tunneling conductance oscillations were observed as shown in Fig. 11. These oscillations depended on the middle layer thickness and the outer electrode magnetization configuration. These oscillations were interpreted as due to the modulation of tunneling conductance by the spin-polarized quantum well states created in the majority Δ_1 state of the middle Fe (001) layer. This study of the quantum size effect in the epitaxial magnetic tunnel junctions indicates great potential for the development of the spin-dependent resonant tunneling effect in coherent tunneling regime.

4. Novel Device Possibilities

The very high TMR value and its small bias dependence are ideal for spintronics applications. One should be able to build devices with extremely high sensitivity and switching speed. Besides MRAM and hard drive read head applications, the huge TMR in MgO based MTJs is useful for other new spintronic devices as well. Diao *et al.* [35] demonstrated magnetization reversal by spin injection using FeCoB/MgO/FeCoB junctions with a TMR of 150% as shown in Fig. 12. They observed a switching current density in the range of 2-3 × 10^6 A/cm^2 which was 3-4 times smaller than those for comparable Al_2O_3 barrier MTJs. This they attributed to higher tunneling spin polarization in the case of MgO junctions. In addition, from the bias dependence studies for both types of MTJs, they qualitatively explained that the lowered P at finite bias was responsible for the

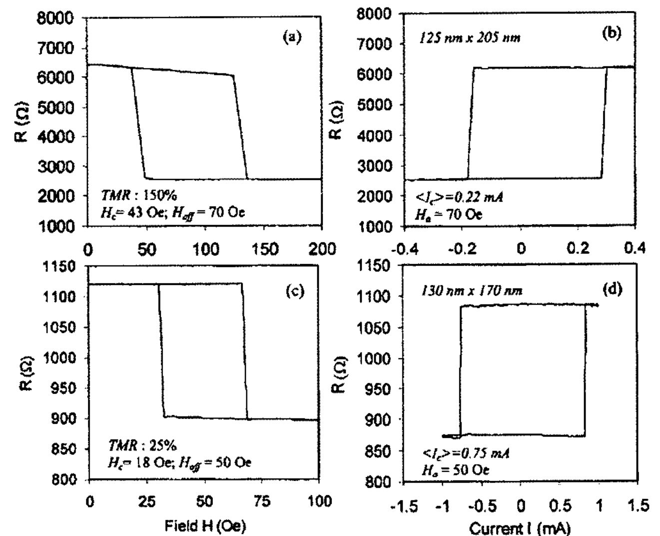

Fig. 12. Magnetization switching shown for an MTJ sample with an MgO barrier taken at room temperature: field (a) and current (b) driven. In comparison, magnetization switching for an MTJ sample with an Al_2O_3 barrier is also shown: field (c) and current (d) driven. 30 ms current pulse width was used in obtaining (b) and (d). From Ref. 35.

suppression of current-driven magnetization switching compared to zero-bias.

Similarly, to investigate the relationship between spin transfer and TMR under finite bias, Fuchs *et al.* utilized the spin-torque response of CoFe/MgO/CoFe junctions having ultrathin MgO tunnel barrier layers [36]. They found that the spin torque per unit current exerted on the free layer decreased by < 10% over a bias range where the TMR decreased by > 40%. From this result they pointed the inconsistency of free-electron-like spin-polariz-ed tunneling and reduced-surface-magnetism models of the TMR bias dependence, whereas it appeared to be consistent with magnetic-state-dependent decay lengths in the tunnel barrier. Highly spin-polarized current in MTJs with MgO would make it possible to reduce the critical current to switch the magnetization. This effect, called spin torque effect, is one of the key parameters for technologically realizing gigabit MRAM.

Recently a novel device was proposed by Tulapurkar *et al.* [37], which is called "spin-torque diode" (Fig. 13(a)). When proper frequency-ac current is input in a small MTJ, the diode output is a dc voltage (Fig. 13(b)). This phenomenon arises from spin-torque effect. When ac current near FMR frequency of the free layer is applied to the MTJ, it exerts a spin torque on the free layer spin moments. The spin is tilted towards the pinned-layer magnetization during the negative (or positive) half of the alternating current due to spin-torque effect. While in

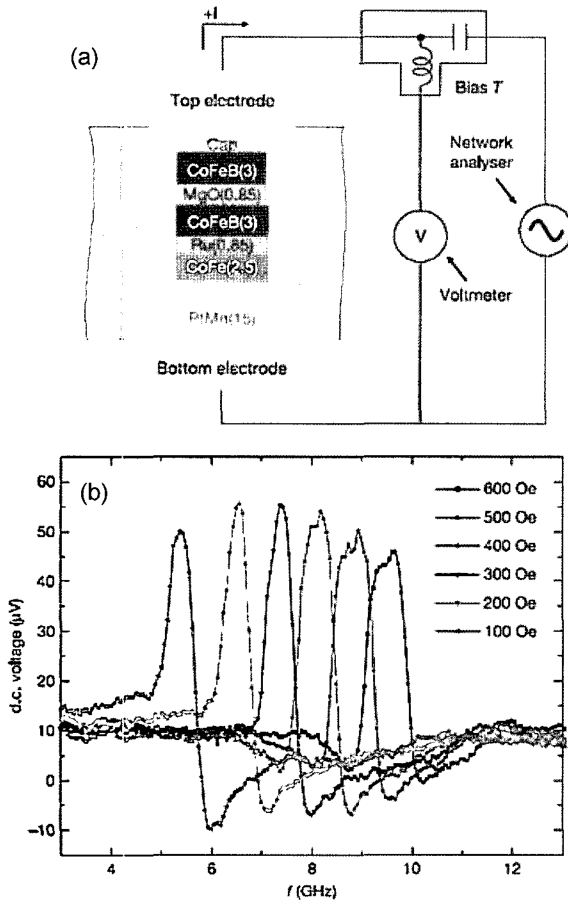

Fig. 13. (a) Schematic diagram of the experimental set-up and cross-sectional view of the magnetic tunnel junction (MTJ) device. The thicknesses of various layers of the device in nanometres are given in brackets. (b) The d.c. voltage is plotted as a function of the frequency of the a.c. current (0.55 mA). The external magnetic fields are as shown. The d.c. voltage results from the resonant oscillation of the magnetic moment of the free layer by current-induced spin-transfer and effective-field torques. From Ref. 37.

another half of ac, free-layer spin moments tilt in opposite direction. The resistance in former half of ac is lower than that in later half because of TMR effect, meaning the resistance alternates in tune with the current. Consequently, the voltage, which is the product of current and resistance, shows finite average value as a dc voltage. The schematic illustration of this mechanism is shown in Fig. 14. Since high TMR ratio makes the output voltage large, MTJs with MgO barrier are ideal junctions for this device. In fact, Tulapurkar *et al.* used CoFeB/MgO/CoFeB junctions to demonstrate the effect.

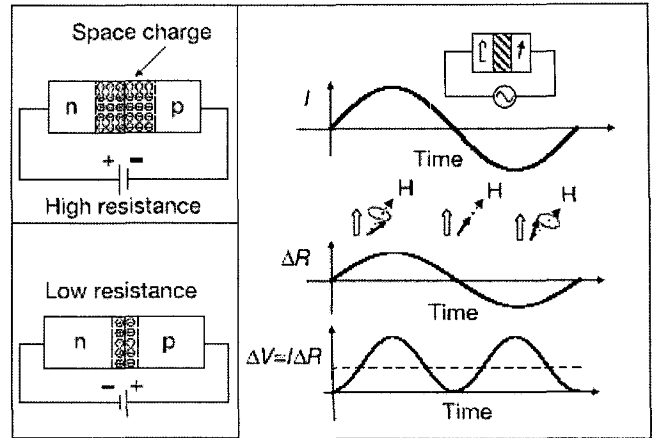

Fig. 14. Principle of the spin-torque diode. a, Comparison of the functioning of the semiconductor p-n diode (left panel) and the spin-torque diode (right panel). In the semi-conductor diode, if positive voltage is applied to the n side, the resistance is high. For the opposite polarity, the resistance is low. In the case of the spin-torque diode, the free-layer magnetization (shown by thin black arrows) oscillates owing to the current-induced torque. The resistance of the diode is less when the ac current is negative, because the free layer makes a smaller angle with the pinned layer (shown by the thick blue arrow). When the ac current is positive, the resistance is larger, owing to the larger angle. The bottom trace in the right panel shows the schematic variation of the product of the current and the change in resistance. The dotted line shows the average value of this product, which appears as dc voltage across the spin-torque diode. From Ref. 37.

5. Conclusions

In the last five years, and especially in the past two years, a large number of epitaxial MTJs with MgO barriers have been studied. Many interesting results have come out. Most notable among them is the observation of very high TMR in epitaxial barrier junctions. It is one of those good moments in the field where the theoretical predictions have led to effective experimental discoveries. The already bubbling field of spin tunneling has been invigorated further by the exciting results obtained with epitaxial MgO barriers. As mentioned above, the field is rich in physics that is still to be explored. There must be many other systems which have the possibilities to surprise even the most conservative ones in the field. There is realistic and enormous potential to realize nanoscale, fast and highly energy efficient devices for the future technology. Many new spintronic devices using MgO barrier should appear in near future.

Acknowledgements

The authors wish to thank NSF, ONR and MIT-KIST programs for the funding support. TN wishes to thank AIST funding for his stay at MIT.

References

[1] J. S. Moodera and R. H. Meservey, in "Magnetoelectronics", Chap. 3, Edited by M. Johnson (Elsevier Academic Press, Boston, 2004).

[2] B. Dieny, Chap. 2; J. Daughton, Chap. 4; J. Akerman *et al.*, Chap. 5 and M. Johnson, Chap. 6 in "Magneoelectronics", Edited by M. Johnson (Elsevier Academic Press, Boston, 2004).

[3] P. P. Freitas, "Magneoelectronics", Chap. 7, Edited by M. Johnson (Elsevier Academic Press, Boston, 2004).

[4] R. H. Meservey and P. M. Tedrow, Phys. Repts. **238**, 173 (1994).

[5] J. S. Moodera, L. R. Kinder, T. M. Wong, and R. Meservey, Phys. Rev. Lett. **74**, 3273 (1995).

[6] T. Miyazaki and N. Tezuka, J. Mag. Mag. Mater. **139**, L231 (1995).

[7] J. M. de Teresa, A. Barthélémy, A. Fert, J. P. Contour, R. Lyonnet, F. Montaigne, P. Seneor, and A. Vaurès, Phys. Rev. Lett. **82**, 4288 (1999).

[8] Z. Li, C. de Groot, and J. S. Moodera, Appl. Phys. Lett. **77**, 3630 (2000).

[9] D. Wang, C. Nordman, J. M. Daughton, Z. Qian, and J. Fink, IEEE Trans. Magn. **40**, 2269-2271 (2004): J.-H. Lee, K.-I. Jun, and J. S. Moodera, unpublished TMR data at LHe temperatures (2004).

[10] Ph. Mavropoulos, N. Papanikolaou, and P. H. Dederichs, Phys. Rev. Lett. **85**, 1088 (2000).

[11] W. H. Butler, X.-G. Zhang, T. C. Schulthess, and J. M. Maclaren, Phys. Rev. B **63**, 054416 (2001).

[12] J. Mathon and A. Umerski, Phys. Rev. B **63**, 220403R (2001).

[13] X.-G. Zhang and W. H. Butler, Phys. Rev. B **70**, 172407 (2004).

[14] B. D. Yu and J.-S. Kim, Phys. Rev. B **73**, 125408 (2006).

[15] C. Heiliger, P. Zahn, B. Yu Yavorsky, and I. Mertig, Phys. Rev. B **72**, 180406 (2005).

[16] J. S. Moodera and L. R. Kinder, J. Appl. Phys. **79**, 4724 (1996).

[17] M. Bowen, V. Cros, F. Petroff, A. Fert, C. Martinez Boubeta, J. L. Costa-Kramer, J. V. Anguita, A. Cebollada, F. Briones, J. M. de Teresa, L. Morellon, M. R. Ibarra, F. Guell, F. Peiro, and A. Cornet, Appl. Phys. Lett. **79**, 1655 (2001).

[18] J. Faure-Vincent, C. Tiusan, E. Jouguelet, F. Canet, M. Sajieddine, C. Bellouard, E. Popova, M. Hehn, F. Montaigne, and A. Schuhl, Appl. Phys. Lett. **82**, 4507 (2003).

[19] H. I. Meyerheim, R. Popescu, N. Jedrecy, M. Vedpathak, M. Sauvage-Simkim, R. pinchaux, B. Heinrich, and J. Kirschner, Phys. Rev. B **65**, 144433 (2002).

[20] W. Wulfhekel, M. Klaua, D. Ullmann, F. Zavaliche, and J. Kirschner R. Urban, T. Monchesky, and B. Heinrich, Appl. Phys. Lett. **78**, 509-511 (2001).

[21] M. Klaua, D. Ullmann, J. Barthel, W. Wulfhekel, J. Kirschner, R. Urban, T. L. Monchesky, A. Enders, J. F. Cochran, and B. Heinrich, Phys. Rev. B **64**, 134411 (2001).

[22] S. Yuasa, A. Fukushima, T. Nagahama, K. Ando, and Y. Suzuki, Jpn J. Appl. Phys. **43**, L588-L590 (2004).

[23] S. Yuasa, T. Nagahama, A. Fukushima, Y. Suzuki, and K. Ando, Nature Mater. **3**, 868 (2004).

[24] S. S. P. Parkin, C. Kaiser, A. Panchula, P. M. Rice, B. Hughes, M. Samant, and S.-H. Yang; Nature Mater. **3**, 862 (2004).

[25] S. Yuasa, A. Fukushima, H. Kubota, Y. Suzuki, and K. Ando, Appl. Phys. Lett. **89**, 042505 (2006).

[26] D. D. Djayaprawira, K. Tsunekawa, M. Nagai, H. Maekawa, S. Yamagata, N. Watanabe, S. Yuasa, Y. Suzuki, and K. Ando, Appl. Phys. Lett. **86**, 092502 (2005).

[27] S. Ikeda, J. Hayakawa, Y. M. Lee, T. Tanikawa, F. Matsukura, and H. Ohno, J. Appl. Phys. **99**, 08A907 (2006); J. Hayakawa, S. Ikeda, Y. M. Lee, F. Matsukura, and H. Ohno, Cond. Mat_0610526.

[28] J. Y. Bae, W. C. Lim, H. J. Kim, D. J. Kim, K. W. Kim, T. W. Kim, and T. D. Lee, J. of Magnetics **11**, 25-29 (2006).

[29] Y. M. Lee, J. Hayakawa, S. Ikeda, F. Matsukura, and H. Ohno, Appl. Phys. Lett. **89**, 042506 (2006).

[30] T. Marukama, T. Ishikawa, K.-I. Matsuda, T. Uemura, and M. Yamamoto, J. Appl. Phys. **99**, 08A904 (2006); Appl. Phys. Lett. **88**, 262503 (2006).

[31] P. G. Mather, J. C. Read, and R. A. Buhrman, Phys. Rev. B **73**, 205412 (2006).

[32] Y. Ando, T. Miyakoshi, M. Oogane, T. Miyazaki, H. Kubota, K. Ando, and S. Yuasa, Appl. Phys. Lett. **87**, 142502 (2005).

[33] C. Tiusan, J. Faure-Vincent, C. Bellouard, M. Hehn, E. Jouguelet, and A. Schuhl, Phys. Rev. Lett. **93**, 106602 (2004).

[34] T. Nozaki, N. Tezuka, and K. Inomata, Phys. Rev. Lett. **96**, 027208 (2006).

[35] Z. Diao, D. Apalkov, M. Pakala, Y. Ding, A. Panchula, and Y. Huai, Appl. Phys. Lett. **87**, 232502 (2005).

[36] G. D. Fuchs, J. A. Katine, S. I. Kiselev, D. Mauri, K. S. Wooley, D. C. Ralph, and R. A. Buhrman, Phys. Rev. Lett. **96**, 186603 (2006).

[37] A. A. Tulapurkar, Y. Suzuki, A. Fukushima, H. Kubota, H. Maehara, K. Tsunekawa, D. D. Djayaprawira, N. Watanabe, and S. Yuasa, Nature 438 339 (2005).